AIAA JOURNAL
Vol. 41, No. 6, June 2003

Approximate Modal Identification of Lightly Damped, Highly Symmetric Bladed Disks

S. J. DiMaggio* and Z. H. Duron†
The Aerospace Corporation, Los Angeles, California 90009-2957
and
G. Davis‡
The Boeing Company, Canoga Park, California 91309-7922

Turbine blade cracking or failure caused by high-cycle fatigue is a concern in both aerospace and aircraft engines. Because of manufacturing advances leading to integrally bladed disks, nonuniformities and damping associated with the blade-to-disk interface have been considerably reduced. In systems such as these, bladed-disk assemblies can behave as lightly damped, rotationally periodic structures in which many resonant conditions, involving response in all of the blades, exist. Because of the nonuniform, aerodynamic forces on the blades, excessive vibration response in the high-frequency regime can be a problem and, thus, identification of resonant conditions in this region of the spectrum is important in avoiding operation at potentially damaging speeds. We present a simple modal identification technique that can help locate potentially harmful resonant conditions and aid in the validation of computational models of highly tuned, bladed-disk assemblies across a wide frequency regime. The experimental approach used to acquire the necessary measurements in a timely manner is also described. An example is presented using data acquired from an impulse test of a turbine and includes results up to 20 kHz.

Nomenclature

b	=	given number of blades
f	=	frequency, Hz
f_n	=	natural frequency, Hz
$H_{i,j}$	=	frequency-response-function relating response at blade i to impact at blade j, g/lbf
H_{ref}	=	frequency response function of reference blade, g/lbf
i	=	blade number
j	=	number of nodal diameters
$\hat{n}$	=	number of nodal diameters for entire disk
n_b	=	number of nodal diameters in b blades
t	=	time, s
t_{ref}	=	arbitrary reference time, s
y_i	=	modal amplitude of blade i
y_{ref}	=	modal amplitude of reference blade
θ_i	=	angular position of blade i, rad
$\phi_{i,j}$	=	phase relating response at blade i to impact at blade j
ϕ_{ref}	=	phase of reference blade, rad

Introduction

PREVENTION of high-cycle fatigue failures, induced by resonant vibration, in turbines is critical in the aerospace, aircraft, and power industries. It is not surprising, therefore, that an extensive amount of research has been directed at understanding and accurately predicting the vibration characteristics of turbine blading.[1–7] Much of this knowledge is derived from analytical models that vary in their ability to treat mistuned conditions and their applicability to predicting response in the high-frequency regime. Regardless of the particular methodologies used, however, the complexity of bladed disk, or blisk, systems suggests that experimental methods be used to verify and validate the theoretical predictions.

This paper presents an expedient (from a test time and postprocessing standpoint) but approximate mode extraction method that can be used across a wide frequency range and requires information that can be acquired using a minimal amount of instrumentation. It is suggested that a single accelerometer, an instrumented force hammer, and a dual-channel data acquisition system are all that is needed in order to conduct impulse response tests from which modal information can be extracted and used to validate complex numerical models and/or Campbell diagrams. Reference 8 provides a thorough explanation of the impulse testing employed to obtain the data required for the modal identification approach documented herein. The experimental technique presented requires an understanding of the well-documented behavior[9–18] of rotationally periodic structures and requires that the blisk be highly tuned and the modes be well separated. Although these restrictions might initially seem rather limiting, the recent introduction of integrally bladed disks with minimal damping and mistuning, in both aerospace and aircraft turbines, seems to make the approach attractive. The effect of mistuning, in which even a small degree of blade-to-blade variability can significantly alter the response characteristics of the hardware, has also been the subject of much research.[19,20]

The approach presented herein for the extraction of blisk response characteristics is not a rigorous modal identification method. Although the authors use the terms "modal identification" and "mode shapes" for brevity, it should be understood that the response shapes identified in this paper are really operating deflected shapes, which, in the case of highly tuned and lightly damped structures, can provide approximate mode shapes that are sufficient for development of Campbell diagrams and provide very useful information for numerical model validation. Furthermore, it is acknowledged that the modal identification approach used herein is rather simplistic compared to some of the more recent and elegant identification strategies. Because of limitations associated with acquiring lightly damped responses over a wide frequency range and a compressed time schedule, the authors elected to use a rather simplistic yet easy-to-implement and easy-to-understand approach that could be

Received 10 September 2001; presented as Paper 2002-1225 at the AIAA/ASME/ASCE/AHS/ASC 43rd Structures, Structural Dynamics, and Materials Conference, Denver, CO, 22–25 April 2002; revision received 1 December 2002; accepted for publication 18 December 2002.

*Project Leader, Environmental Test and Ordnance Department, P.O. Box 92957. Member AIAA.
†Senior MTS, Structural Dynamics Department, P.O. Box 92957. Member AIAA.
‡Senior Engineering Specialist, Development Stress/Advanced Analysis, Rocketdyne Propulsion and Power Division.

employed in practice by any test engineer in an industry, production-line setting.

The accurate extraction of modal characteristics for highly tuned blisks presents many challenges, chief of which is the sensitivity of the structure to perturbations caused by the measurement system. This problem, discussed in Ref. 21, has led most experimentalists to employ relatively unobtrusive measurement schemes, including laser vibrometers,[21,22] strain gauges,[23] fiber-optic sensors,[24] and proximity probes.[25] Additional experimental approaches related to turbines are also discussed in the context of accurately measuring blisk damping values.[26–28] Nevertheless, a systematic approach to experimental verification of complex blisk models is not well established.

Unlike the previous approaches, this paper documents an experimental approach and corresponding approximate modal extraction procedure that relies on an accelerometer to obtain the responses. Special tests, discussed in this paper, were performed to demonstrate that the use of the accelerometer did not induce any significant mistuning into the system and that the blisk behaved as a highly tuned, rotationally periodic structure. Although details are not provided herein because of length restrictions, results obtained using an accelerometer provided improved fidelity as compared to those obtained on the same structure using strain gauges and laser vibrometers.

Background

A blisk and shaft are illustrated in Fig. 1, supported on a special stand used during the tests. As a result of a unique design and manufacturing process, the structural system illustrated in Fig. 1 exhibits extremely low damping and is highly redundant. For example, structural damping values on the order of 0.01% of critical were measured. The term "highly redundant" implies that blade-to-blade variability in material and geometric properties can be considered negligible.

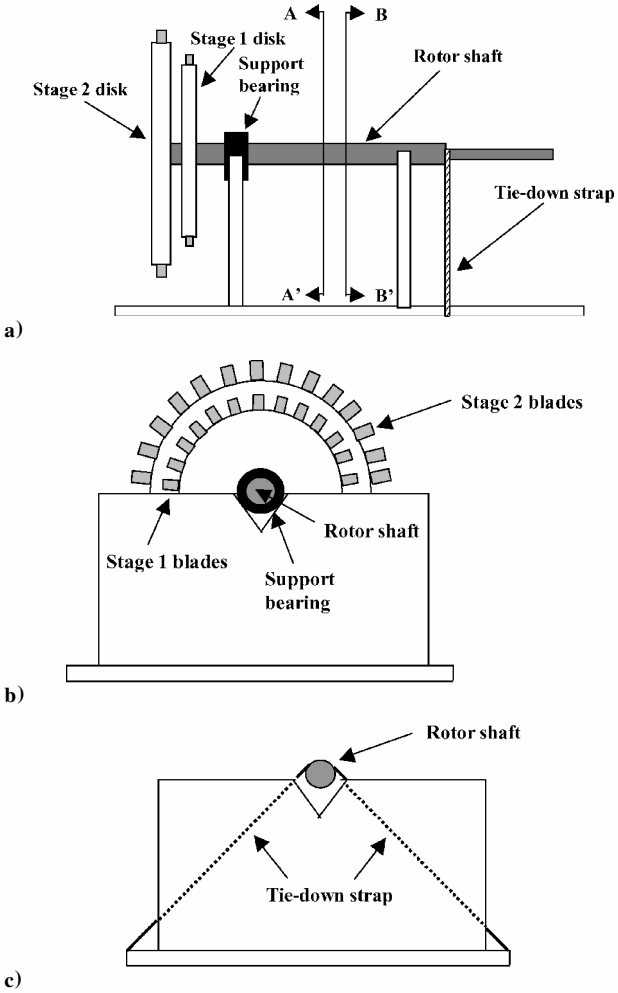

Fig. 1 Turbopump blisk and shaft supported in test stand. a) Stage 1 blades (smaller) and stage 2 (larger) blades are shown at the left end of the blisk assembly. Note the bearing that is seated in the left-hand support; b) section A-A'; and c) section B-B'.

In the case of the tuned turbine rotor, the blade modes of vibration occur in families, or clusters, that are described according to their relationship to responses of a single blade mounted (cantilevered) on a rigid base or, in other words, uncoupled from the disk. For instance, at any particular resonant frequency in which the blades deform relative to the disk the blades exhibit a response shape characteristic of one of the modes of a single, cantilevered blade. All blades around the circumference of the disk, however, do not deform with the same modal amplitude or phase. Rather, the amplitude and phase vary in a periodic manner around the circumference of the disk with a given number of nodal diameters. For a given single, cantilevered-blade mode shape, the number of nodal diameters in the coupled-system mode governs the amplitude and phase relationship between individual blades on the rim. The total number of nodal-diameter manifestations, or diametrals, of each single, cantilevered-blade mode is $m = (N-1)/2$, for N odd, where N is the number of blades. When perfect axial symmetry exists, two "repeated" modes that have the same nodal-diameter shape and are separated by an arbitrary angle exist at each resonant frequency.

For the turbine rotor tested 123 stage-one blades were present, resulting in 61 diametrals for each of the single, cantilevered-blade mode shapes. For a tuned blisk vibrating in a mode having j nodal diameters, the modal amplitude of blade i on the periphery can be expressed as[7]

$$y_i = A \sin(j\theta_i) \cos(2\pi f_n t) \tag{1}$$

for

$$\theta_i = (2\pi/123)(i-1), \qquad i = 1, \ldots, 123 \tag{2}$$

as shown in Fig. 2. The shape of vibration on the periphery of the disk is $A \sin j\theta_i$, and the frequency of the resonant oscillation is denoted f_n.

The drawings in Fig. 2 are intended to illustrate modal response for the first three diametrals. For the first diametral a single nodal-diameter line exists, and the two blade groups located on either side of this node line respond with opposite phase. Although this might be the first diametral, the blade response relative to the disk can be characterized by any of the mode shapes for a single, cantilevered blade. If blades are located exactly on the nodal diameter line, however, they exhibit no response. For a diametral characterized by j nodal-diameter lines, blades located exactly $\phi = 2\pi/j$ radians apart exhibit the same amplitude and phase response behavior. For example, the second diametral corresponds to $j = 2$ and, as shown in Fig. 2, blades separated by $\phi = \pi$ radians exhibit the same amplitude and phase response. As the number of nodal diameters increases, the natural frequencies of the coupled system, or blisk, asymptotically approach the respective cantilevered frequencies of a single blade.

The nomenclature used in this report is introduced by considering what is referred to as the eighth diametral of the third blade mode. This mode shape is denoted as 3(8) and describes a mode characterized by blades that deform relative to the disk in the third cantilevered mode shape. In this mode, the response amplitude and phase of individual blades vary sinusoidally around the blisk circumference with eight full waves.

In the following sections of this paper, the blisk is treated as a perfectly tuned system in which all of the blades are assumed to be identical. In fact, no system is perfectly symmetric, and a small degree of mistuning is always present. This slight variability in blade geometry and material properties causes the "repeated" modes just mentioned to split in frequency. Each nodal diameter shape can, thus, occur at two distinct natural frequencies that deviate by an amount depending on the degree of imperfection in the blisk. In the absence of significant mistuning, as in the case of the hardware discussed herein, these two modes appear either as very closely

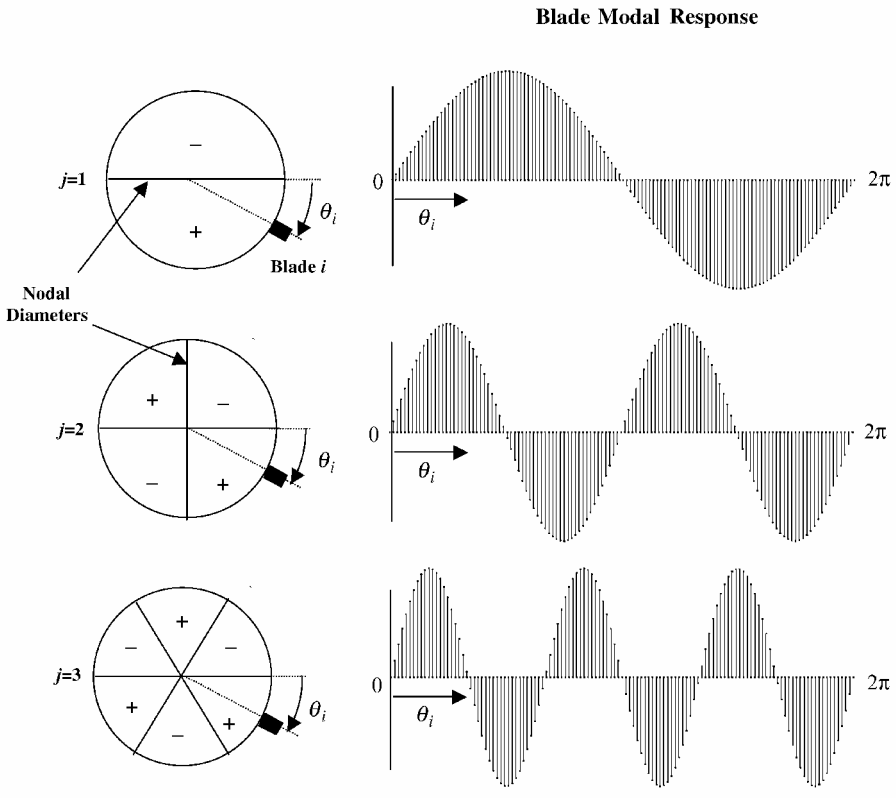

Fig. 2 Vibration modes of a highly tuned bladed disk.

spaced resonances or, depending on the frequency resolution of the frequency response functions (FRFs), as a single resonance. The approach described here assumes that the pairs are, in fact, repeated in frequency and a single approximate mode shape, which is a linear combination of the two modes in the pair, is estimated.

Experimental Approach

The main goal of the experiments described herein was to obtain data necessary to perform an approximate modal identification of the bladed disk portion of the turbopump assembly illustrated in Fig. 1. The test article consisted of the blisk and pump shaft mounted in a specially designed support fixture. The center of mass was located at the blisk end of the test article, thus ensuring that the shaft bearing (Fig. 1) maintained contact with the fixture and that the tie-down strap at the other end of the shaft remained in tension. This setup allowed the blisk to be easily rotated in order to provide access to any particular blade of interest.

Light damping and the relatively large frequency range of interest associated with the blisk response guided the choice of instrumentation and the design of suitable test procedures. It also led to extended acquisition times in order to allow transients to fully decay back to levels present prior to the transient event. The large frequency range of interest (20 kHz) further required unusually small sampling intervals and, together with the extended acquisition times, resulted in large data sets. Although mass loading effects were considered at the onset of testing, the miniature accelerometer used to measure blade response did not significantly affect the measurements or the extracted dynamic characteristics. This finding is based on tests conducted using a laser vibrometer to measure stage-one blade response both with and without the miniature accelerometer mounted. Evaluation of the FRFs revealed that the location of resonant peaks remained unaffected in frequency. The ratio of accelerometer mass to blade mass for these tests was 0.004.

Test procedures were based on standard impulse test techniques and were designed to provide reliable and repeatable measurements of impact force and blade response. Although the main purpose of the experiments was to characterize the entire blisk assembly illustrated in Fig. 1, several tests were also conducted on the single-blade test article illustrated in Fig. 3. Thus, whereas the paper will focus on the blisk tests, the single-blade article is used to describe the force and response locations used during both tests.

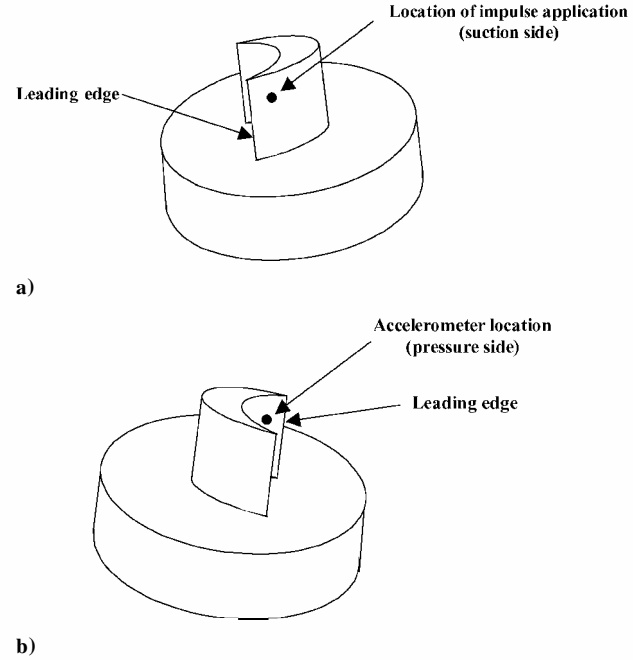

Fig. 3 Accelerometer mounting and impulse locations as shown on single-blade article. For these tests a) impacts were applied on the suction side at the location shown and b) a single accelerometer was attached on the pressure side of the blades at the location shown.

Transient blade response caused by the application of an impact (force pulse) was obtained, using a miniature accelerometer glued to the pressure side of blade 1 on the blisk at the location shown in Fig. 3b (shown on the single-blade test article). Impacts were applied sequentially on stage-one blades on the suction side, as shown in Fig. 3a.

Because of limitations associated with the data acquisition hardware, resulting from the high sample rate and long data records required for these tests, only the force pulse and a single acceleration response could be acquired concurrently. Furthermore, given the requirement to glue the miniature accelerometer to the blades in order to provide high-frequency vibration transmission, it was impractical to consider moving the transducer from blade to blade during the test. As a result, an alternate approach was used in which the transducer remained attached to blade 1 for the duration of the tests, while impacts were applied sequentially to blades 1–24, numbered in a clockwise direction around the circumference of the blisk. This procedure varied from the more desirable practice of applying an impulse, or input, at one location (fixed during test), and monitoring transient response, or output, at all measurement locations simultaneously.

To assess the degree to which symmetry was present in blade response behavior, a special series of tests were performed. In these tests the responses at blade 1 as a result of impacts at blades 1–5 were compared to the responses at blade 20 as a result of impacts at blades 20–24. Similarity in the resulting FRFs indicated that a high degree of blade symmetry was present in the blisk response behavior, thus allowing any location (i.e., any stage one blade) to be used as the reference. In the case of the modal identification procedure discussed in the preceding section, it is, therefore, believed that the approximation of the blisk as a perfectly tuned system is warranted and provides an accurate estimate of the true system behavior.

Spectral estimates were obtained using standard Fourier analysis techniques and included power spectral densities (PSDs), FRFs, and coherence. FRFs were computed using the acceleration at blade 1 as the output and the impulses applied sequentially to the stage-one blades as the inputs. In the following sections of this paper, it is assumed that high-quality FRFs, relating the acceleration response at blade number one to a force input at blades 1–24, for frequencies up to 20 kHz, have been acquired. For a complete discussion of the experimental techniques required to obtain these responses, the reader is again referred to Ref. 8.

FRFs for Single-Blade Test Article

Prior to testing the complete blisk assembly illustrated in Fig. 1, the single-blade test article shown in Fig. 3 was tested. This preliminary test provided the experimentalist a reasonable expectation of where in the frequency spectrum modal clusters associated with each cantilevered-blade mode would exist.

A single-blade FRF magnitude estimate, relating acceleration response to the applied impulsive force, is shown in Fig. 4. The first three resonant peaks for the single-blade test article are easily identified at 10,550, 13,177, and 19,035 Hz, respectively. A finite element model was also generated for the single-blade test article, and the computed natural frequencies in Table 1 (for the first three modes) show good correlation with the experimental results. The results of the numerical model for the single blade, with the flexible base removed and a cantilevered boundary condition imposed, are also shown in Table 1.

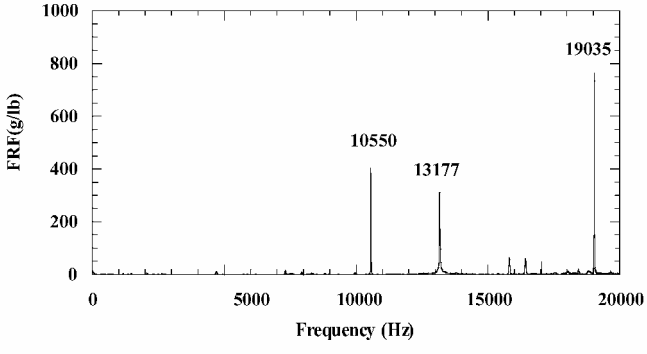

Fig. 4 FRF magnitude for single-blade test article.

Table 1 Summary of single-blade frequencies

Mode	Experimental frequency	Numerical model flexible base frequency	Numerical model cantilevered frequency
1	10,550	10,551	11,868
2	13,177	13,181	14,442
3	19,035	19,000	21,176

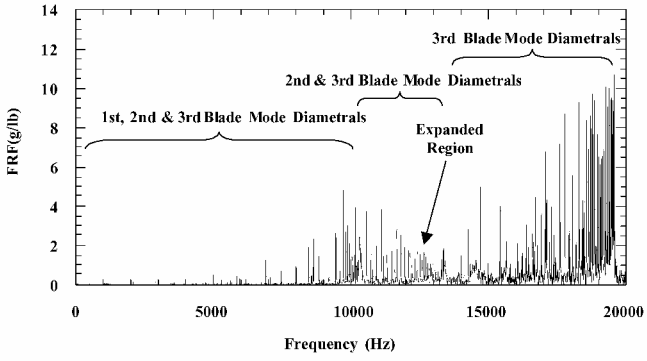

Fig. 5 FRF magnitude relating blisk response at blade 1 to impulse applied at blade 1.

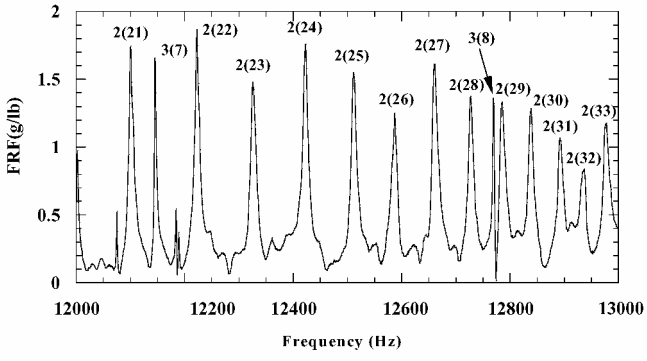

Fig. 6 Expanded view of Fig. 5.

FRFs for Complete Blisk

The FRF shown in Fig. 5 was determined from the full-blisk tests and relates acceleration response at blade 1 as a result of an impulse applied to blade 1. Blade measurement locations (for both impact and response) were the same as those employed during the single-blade tests.

Comparison of the FRF magnitude in Fig. 5 with the single-blade results shown in Fig. 4 reveals significant differences in spectral character. Whereas the single-blade FRF magnitude contains three dominant resonances, associated with blade bending and torsional behavior, the strong coupling between the blades on the blisk rim leads to the appearance of many closely spaced resonances in the full-blisk system. The FRF magnitude in Fig. 5 is characterized by the presence of three clusters, or families, of blade modes. In each cluster the blade-mode diametrals are observed to asymptotically approach frequencies of 10,335, 13,408, and 19,595 Hz, respectively. As expected, these frequencies are all below the cantilevered frequencies summarized in Table 1.

Figure 6 shows an expanded view of the designated region shown in Fig. 5. From the information in Table 1 and an understanding of the well-documented behavior of highly tuned bladed disks, the probable mode shapes associated with the resonant peaks shown in Fig. 6 can be inferred. As indicated in Fig. 5, the resonant peaks associated with the higher-order, cantilevered-blade modes can be interspersed with the lower-order, cantilevered mode shapes. For example, although the closely spaced peaks at 12,772 and 12,786 Hz might, in other structural systems, be interpreted as a split-second mode resonance, mode-extraction techniques reveal the 12,772 resonance to be the eighth diametral of the third blade mode. Conversely,

none of the first blade-mode diametrals exist above the associated cantilever frequency of 11,868 Hz and, thus, are not evident in Fig. 6.

Approximate Mode Extraction

The FRFs acquired during test related the response at blade 1 (reference measurement location) to impacts applied sequentially to each blade tested. Maxwell's reciprocal theorem suggests that the FRFs relating acceleration response at blade 1 to impulses applied at blades $j = 1, \ldots, 24$ can be considered to be identical to FRFs relating the acceleration at blades $i = 1, \ldots, 24$ to an impulse applied at blade 1. (Applying Maxwell's reciprocal theorem to this test procedure implies that the response at blade i caused by a force applied at blade j is equal to the response at blade j caused by a force applied at blade i.) With this result blisk mode shapes can be identified on the basis of the measured FRFs and the assumed sinusoidal character of blade response at a single resonant frequency.

For an arbitrary time t and a given frequency f, the response at each blade tested, as a result of an impulse applied at blade 1, is expressed by

$$y_i(t, f) = |H_{i,1}(f)| \sin[2\pi f t + \phi_{i,1}(f)] \tag{3}$$

where $|H_{i,1}(f)|$ and $\phi_{i,1}(f)$ are the FRF magnitude and phase of the response at blade $i = 1, \ldots, 24$, as a result of an impulse at blade 1. By virtue of Maxwell's theorem, these quantities are equivalent to the measured FRF magnitude and phase $|H_{1,i}(f)|$ and $\phi_{1,i}(f)$ acquired by measuring the response at blade 1 as a result of impulses applied sequentially to blades 1–24.

Of the 24 blades tested, any one of them can be arbitrarily selected so that its estimated modal response amplitude is equal to its

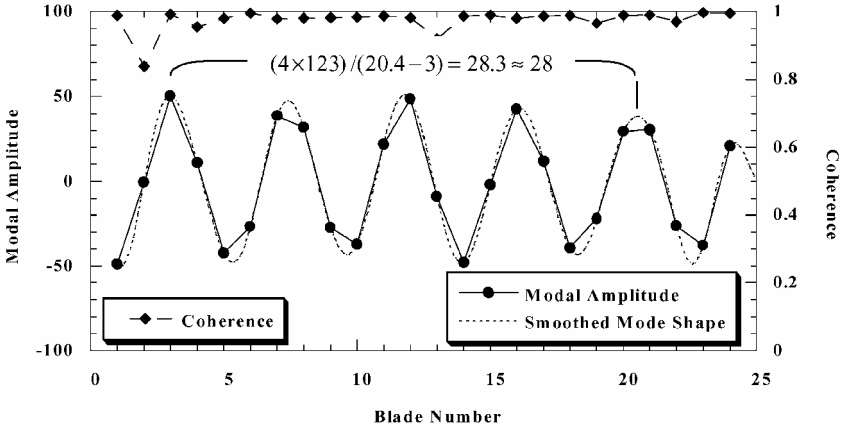

a) 2(28) mode at 12,728 Hz

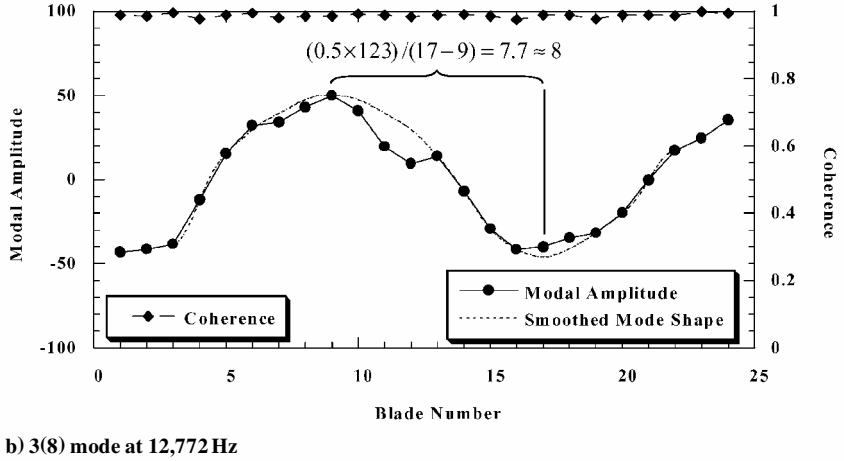

b) 3(8) mode at 12,772 Hz

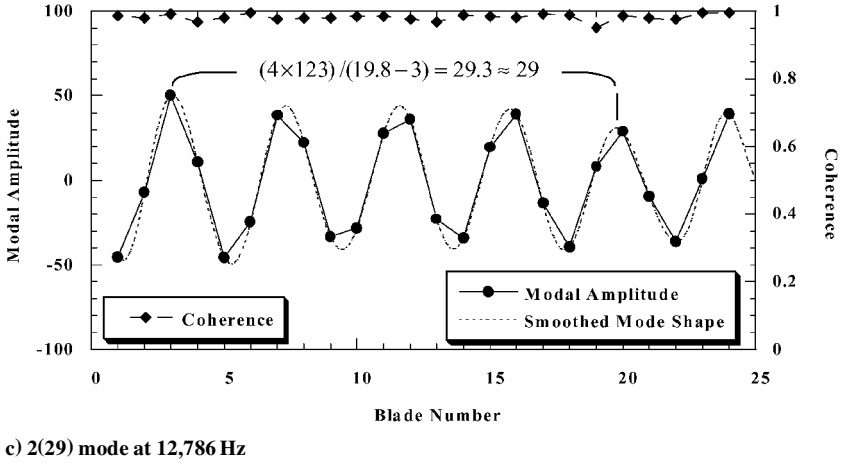

c) 2(29) mode at 12,786 Hz

Fig. 7 Response shapes corresponding to 2(28), 3(8), and 2(29) modes.

FRF magnitude estimate. For a particular resonant frequency f_n this location is taken as the reference location, where

$$y_{\text{ref}}(f_n) = |H_{\text{ref}}(f_n)| \tag{4}$$

$$\sin[2\pi f_n t + \phi_{\text{ref}}(f_n)] = 1 \tag{5}$$

By virtue of Eq. (5), this response occurs at the arbitrary time

$$t = t_{\text{ref}} = (1/2\pi f_n)(\pi/2 - \phi_{\text{ref}}) \tag{6}$$

The responses of all other blades can now be synchronized in time by setting $t = t_{\text{ref}}$ in Eq. (3), and their resulting modal response estimates are computed as

$$y_i(t_{\text{ref}}, f_n) = |H_{1,i}(f_n)| \sin[2\pi f_n t_{\text{ref}} + \phi_{1,i}(f_n)] \tag{7}$$

Although the ratios of these modal amplitudes characterize the unique shape of the modal response, their amplitudes can be scaled by any factor necessary for visualization. In the case of these tests, a scale factor of 50 was used to obtain the modal plots contained herein.

Using this procedure, response shapes associated with the blade resonances at 12,728, 12,772, and at 12,786 Hz were identified and are shown in Fig. 7. In each of the plots shown, the abscissa indicates the blades from 1 to 24, whereas the ordinate indicates the corresponding modal amplitudes $y_i(t_{\text{ref}}, f_n)$. Computed blade modal amplitudes are denoted by the solid dots connected by straight solid lines, and a "smoother" result, obtained through a spline fit, is also shown. In both cases, however, the nature of the mode shape is preserved, and the periodic pattern is what an observer would see at an instant of time, in the plane of the disk, if the circumference were "unwrapped," or laid out in a straight line. Uniformly high coherence values, associated with the FRF estimates (at the particular frequency under consideration) for each individual blade, are denoted by diamonds connected by solid lines.

Because these mode-shape plots contain information for the first 24 blades only, a determination of the number of nodal diameters for the entire disk is obtained by

$$\hat{n} = 123 n_b / b \tag{8}$$

The ratio n_b/b is the number of nodal diameters per blade, which, when multiplied by 123 (total number of stage-one blades), yields the number of nodal diameters present in the blisk. In this manner the number of blisk nodal diameters can be identified from responses acquired over a portion of the blisk. For example, in Fig. 7a, using the smoothed mode shape curve, $n_b = 4$ nodal diameters were observed over $b = (20.4 - 3) = 17.4$ blades, yielding $\hat{n} = (4 \times 123)/(20.4 - 3) = 28.3$ or, approximately, 28 diametrals present in the entire disk. Similar calculations are also shown in Figs. 7b and 7c for the 3(8) and 2(29) modes. Note that the smoothed curve was used in order to obtain a fractional number of blades b, rather than simply using the integer number of blades in the physical system. This allowed the resonant peaks at 12,728, 12,772, and 12,786 Hz (shown in Fig. 6) to be identified as the 2(28), 3(8), and 2(29) modes of the blisk.

Examination of the FRF curve in Fig. 6 reveals a pattern in which the spacing between the majority of resonant peaks appears to decrease with increasing frequency. This is characteristic of the fact that the natural frequencies of the second-blade-mode family asymptotically approach the corresponding cantilever frequency, estimated by the single-blade, cantilevered model to be 14,442 Hz. Identifying the number of diametrals associated with a single resonant peak in the family, therefore, is often sufficient to infer the number of nodal diameters associated with the remaining resonances. For example, if the mode extraction process identifies the 2(29) and 2(33) modes in Fig. 6 it is reasonable to infer that the three intermediate peaks correspond to the 2(30), 2(31), and 2(32) modes. The exception in the trend is the response at 12,772 Hz, which was presumed to be a diametral associated with the third blade-mode family on the basis of an initial visual inspection of the FRF. By virtue of the response shape shown in Fig. 7b, this resonant peak was subsequently determined to be the 3(8) blade mode. Closer examination of the FRF over a wider frequency range indicates that the response at 12,772 Hz, while being interspersed with second-mode diametrals, does fall into a similarly ordered numerical pattern that characterizes the third blade-mode family.

Identification of blade modal responses using Eqs. (3–8) has been shown to yield reasonable estimates of mode shapes for applications where the measured FRFs are characterized by well-spaced resonant behavior. For example, the FRF magnitude in Fig. 6 shows a resonance at 12,728 Hz that is fairly well isolated from neighboring peaks, whereas the response at 12,772 Hz, however, is influenced by the peak at 12,786 Hz. This coupling manifests itself in the corresponding mode shape plots by the presence of kinks, or deviations, from an otherwise smooth response shape. This is illustrated in the 3(8) mode shape shown in Fig. 7b. The spline curve fit shows a smooth shape that is characteristic of the 3(8) mode, whereas the measured FRF data (denoted by solid dots and solid, linear connecting lines) show a deviation from a purely periodic pattern at blades 10–12.

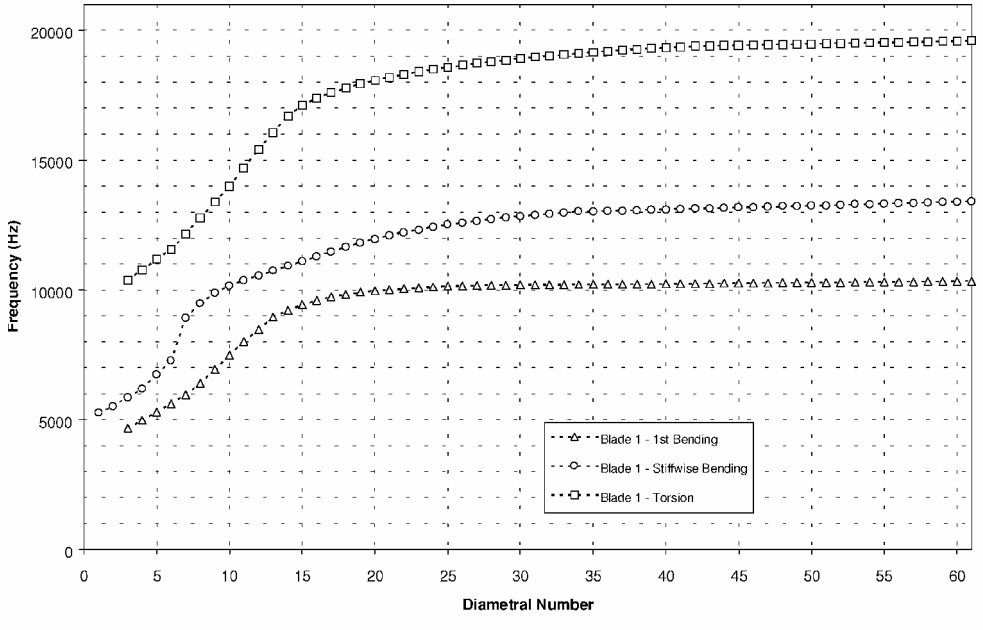

Fig. 8 Blisk natural frequency chart for first three blade-mode families.

Table 2 Third blade-mode natural frequencies

Diametral number	Natural frequency	Diametral number	Natural frequency
1	ND[a]	31	18,967[b]
2	ND	32	19,014[c]
3	10,377	33	19,065[b]
4	10,778	34	19,111[b]
5	11,179[c]	35	19,151[c]
6	11,580[c]	36	19,193[b]
7	12,147[c]	37	19,230[b]
8	12,772[c]	38	19,264[b]
9	13,383	39	19,299[c]
10	13,994[c]	40	19,329[c]
11	14,708[c]	41	19,355[b]
12	15,425[c]	42	19,386[c]
13	16,064[b]	43	19,397
14	16,699[b]	44	19,408
15	17,109[c]	45	19,419
16	17,390[b]	46	19,430
17	17,603[c]	47	19,441
18	17,777[c]	48	19,452
19	17,934[b]	49	19,463
20	18,068[b]	50	19,474
21	18,185[b]	51	19,485
22	18,300[b]	52	19,496
23	18,394[b]	53	19,507
24	18,485[c]	54	19,518
25	18,572[b]	55	19,529
26	18,649[b]	56	19,540
27	18,719[b]	57	19,551
28	18,789[b]	58	19,562
29	18,849[b]	59	19,573
30	18,911[b]	60	19,584
		61	19,595[b]

[a] Not determined.
[b] Identified by inspection of FRF.
[c] Identified with mode extraction technique. All others linearly interpolated.

System Identification

The process described in the preceding section was carried out for a number of FRF peaks so that, in conjunction with the deterministic nature of highly tuned blisk behavior, the response shapes associated with each structural resonance could be identified for the first three families of blade modes. Results are presented in Fig. 8 in which the natural frequencies of the first three-blade-mode families are plotted vs the number of diametrals in the response shape.

Table 2 summarizes the manner in which data points, associated with the third cantilevered blade-mode family, shown in Fig. 8, were identified. The numbers with the superscript c indicate that the extraction technique summarized in Eqs. (3–8) was used to identify the response shapes, numbers with the superscript b indicate that visual inspection of the FRF was used, and numbers with no superscript indicate that the frequencies were linearly interpolated between other, adjacent frequencies. Note that all modes identified with the extraction technique (superscript c) were verified using a visual inspection of the FRF (superscript b). Modes with fewer than three diametrals were not identified for the third blade-mode cluster. To provide a rigorous determination of the lower-order diametrals, more than 24 blades should be processed in order to obtain a full wavelength around the circumference of the disk. In Fig. 8 and Table 2, however, many of the lower-order blade-mode diametrals, although interspersed with disk modes in the low-frequency region, were estimated by extrapolating back in frequency from higher-order, blade-mode diametrals that were obtained with a high degree of confidence. Taken together, Figs. 7 and 8 and Table 2 represent a summary of the system identification procedure used on the blisk.

Damping Estimates

Damping estimates for stage-one blade response, for each of the three blade-mode families, were obtained using the half-power method. PSD functions were used in conjunction with a zero-padding[29] preprocessing step, in which the time histories were padded with an appropriate number of zeros, in order to obtain finer spectral resolution. As a result, although the original PSD estimates contained a 0.76-Hz resolution that was not deemed sufficient for the half-power method, zero padding led to an enhanced resolution of 0.11 Hz. The enhanced resolution allowed a series of estimates, for a wide range of resonant peaks in the three blade-mode families, to be obtained. Figure 9 shows the damping estimates (denoted by solid diamonds) for specific spectral peaks in each of the three blade-mode families. Although the damping estimates for each of the three blade-mode families show some variation with frequency, overall magnitudes remain fairly small and do not exceed 0.025% of critical. The relative stability in these estimates, within each blade-mode family, can be taken as an indication of the reasonableness of the half-power method as applied to the enhanced spectral estimates.

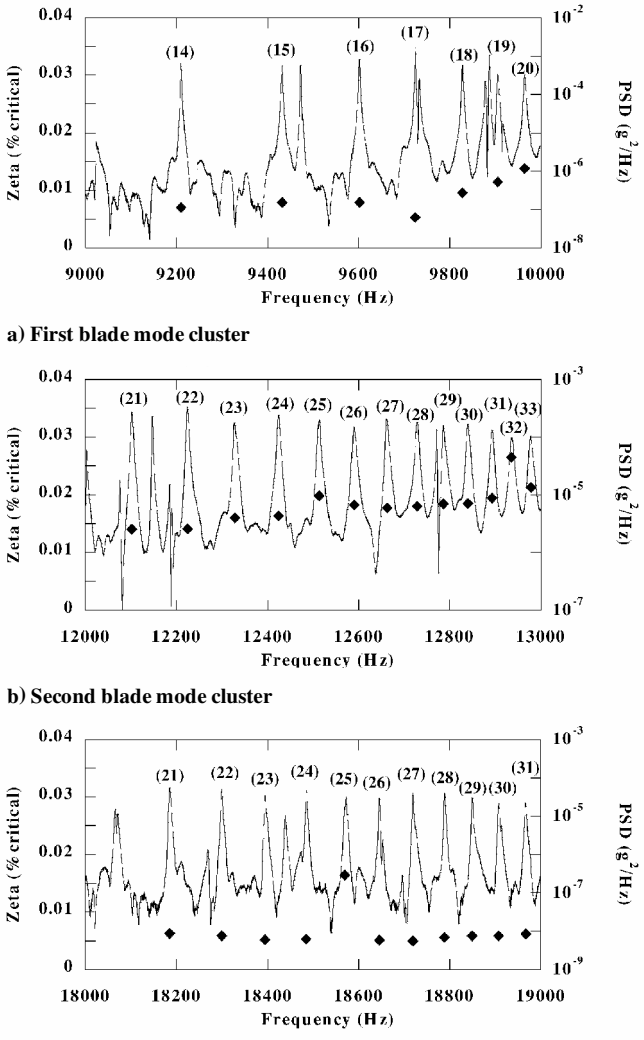

a) First blade mode cluster

b) Second blade mode cluster

c) Third blade mode cluster

Fig. 9 Damping estimates shown in percent of critical by ◆ and referred to the left-hand ordinate for each of the three blade clusters, and ——, the PSDs referred to the right-hand ordinate.

It should be understood that using the half-power method to obtain damping values for the blisk is an approximation that relies on the assumption of perfect symmetry and an absence of very closely spaced modes that can be present in slightly mistuned systems. The estimates presented in this section were, therefore, checked using more rigorous damping extraction techniques[30] that are not discussed herein. The damping estimates obtained from the other methods investigated provided results that confirm the approximations presented in this section.

For the estimates presented in Fig. 9, if split peaks were observed in the FRFs the data points for the corresponding damping values were higher than those obtained for the single peaks. For example,

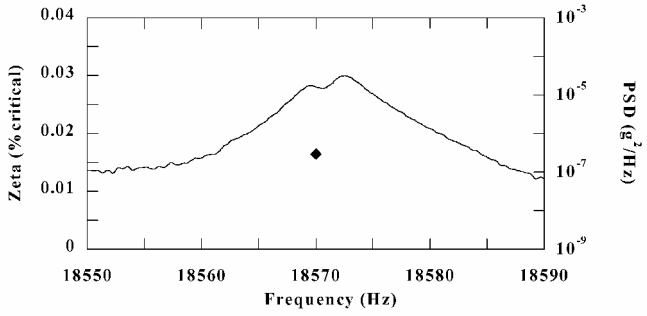

Fig. 10 Twenty-fifth diametral of the third blade mode showing a split peak and its effect on the damping estimate.

the 3(25) mode, shown in Fig. 9c, is shown on a different scale in Fig. 10. Note the split peak in Fig. 10 and the corresponding damping value in Fig. 9c that is slightly higher than the rest of the third blade-mode cluster. Finally, if any modes associated with higher-order blade clusters were interspersed in the plots intended to show estimates for a lower-order blade cluster, the corresponding damping values were omitted.

Conclusions

A method has been proposed to extract modal information from highly symmetric, lightly damped bladed disks. The attractiveness of the method lies in its simplicity and the ease in which the results can be interpreted. The method is particularly useful for turbine rotors with lightly damped, stiff blades. These cases require modal identification into the high-frequency regime and, therefore, very high sampling rates and long data records. Finally, it is suggested that, compared to more rigorous and established mode-survey-type identification methods, the data required to employ the method described herein can be gathered efficiently and in a timely manner. Although it is acknowledged that the proposed method has certain limitations compared to traditional methods (i.e., true mode shapes are not extracted), in a compressed schedule the technique can, indeed, help locate potentially harmful resonant conditions in bladed disks and aid in the validation of complex computational models.

Acknowledgments

This work was supported by Space and Missile Systems Center, Air Force Space Command under Contract F04701-00-C-0009. The authors thank Chafic Hammoud, Myun Kim, and Erwin Perl for their contributions to the computational work discussed herein.

References

[1]Campbell, W., "The Protection of Steam-Turbine Disk Wheels from Axial Vibration," American Society of Mechanical Engineers, Paper 31-160, May 1924.

[2]Ewins, D., "Vibration Characteristics of Bladed Disc Assemblies," *Journal of Mechanical Engineering Science*, Vol. 15, No. 3, 1973, pp. 165–186.

[3]Tobias, S. A., and Arnold, R. N., "The Influence of Dynamical Imperfection on the Vibration of Rotating Disks," *Proceedings of the Institution of Mechanical Engineers*, Vol. 171, 1957, pp. 669–690.

[4]Ewins, D. J., and Srinivasan, A. V., "Vibrations of Bladed Disk Assemblies," Ninth Biennial Conf. on Mechanical Vibration and Noise, American Society of Mechanical Engineers, New York, Sept. 1983.

[5]Srinivasan, A. V. (ed.), *Structural Dynamic Aspects of Bladed Disk Assemblies*, American Society of Mechanical Engineers, New York, 1976.

[6]Leissa, A. W., MacBain, J. C., and Kielb, R. E., "Vibrations of Twisted Cantilevered Plates—Summary of Previous and Current Studies," *Journal of Sound and Vibration*, Vol. 96, No. 2, 1984, pp. 159–173.

[7]Srinivasan, A. V., "Vibrations of Bladed Disk Assemblies—A Selected Survey," *Journal of Vibration, Acoustics, Stress, and Reliability in Design*, Vol. 106, April 1984, pp. 165–168.

[8]Duron, Z. H., and DiMaggio, S. J., "High Frequency Impulse Testing of Lightly-Damped Turbine Disks," AIAA Paper 2002-1532, April 2002.

[9]Ahmad, S., Anderson, R. G., and Zienkiewicz, O. C., "Vibration of Thick Curved Shells, with Particular Reference to Turbine Blades," *Journal of Strain Analysis*, Vol. 5, No. 3, 1970, pp. 200–206.

[10]Dokainish, M. A., and Rawtani, S., "Vibration Analysis of Rotating Cantilever Plates," *International Journal for Numerical Methods in Engineering*, Vol. 3, No. 4, 1979, pp. 233–248.

[11]MacBain, J. C., "Vibratory Behavior of Twisted Cantilevered Plates," *Journal of Aircraft*, Vol. 12, No. 4, 1975, pp. 343–349.

[12]Kielb, R. E., Leissa, A. W., and MacBain, J. C., "Vibrations of Twisted Cantilevered Plates—A Comparison of Theoretical Results," *International Journal for Numerical Methods in Engineering*, Vol. 21, No. 8, 1985, pp. 1365–1380.

[13]Srinivasan, A. V., Lionberger, S. R., and Brown, K. W., "Dynamic Analysis of an Assembly of Shrouded Blades Using Component Modes," *Journal of Mechanical Design*, Vol. 100, July 1978, pp. 520–527.

[14]Mota Soares, C. A., Petyt, M., and Salama, A. M., "Finite Element Analysis of Bladed Disks," *Structural Dynamic Aspects of Bladed Disk Assemblies*, edited by A. V. Srinivasan, American Society of Mechanical Engineers, New York, 1976, pp. 73–91.

[15]Salama, A. M., Petyt, M., and Mota Soares, C. A., "Dynamic Analysis of Bladed Disks by Wave Propagation and Matrix Difference Techniques," *Structural Dynamic Aspects of Bladed Disk Assemblies*, edited by A. V. Srinivasan, American Society of Mechanical Engineers, New York, 1976, pp. 45–56.

[16]Wildheim, J., "Vibrations of Rotating Circumferentially Periodic Structures," *Quarterly Journal of Mechanics and Applied Mathematics*, Vol. 34, Pt. 2, May 1981, pp. 213–229.

[17]Thomas, D. L., "Standing Waves in Rotationally Periodic Structures," *Journal of Sound and Vibration*, Vol. 37, No. 2, 1974, pp. 288–290.

[18]Thomas, D. L., "Dynamics of Rotationally Periodic Structures," *International Journal for Numerical Methods in Engineering*, Vol. 14, No. 1, 1979, pp. 81–102.

[19]Afolabi, D., "The Eigenvalue Spectrum of a Mistuned Bladed Disk," *Vibrations of Blades and Bladed Disk Assemblies; Proceedings of the Tenth Biennial Conference on Mechanical Vibration and Noise*, American Society of Mechanical Engineers, New York, 1985, pp. 23–30.

[20]Wei, S. T., and Pierre, C., "Localization Phenomena in Mistuned Assemblies with Cyclic Symmetry Part 1: Free Vibrations," *Journal of Vibration, Acoustics, Stress, and Reliability in Design*, Vol. 110, No. 4, 1988, pp. 429–438.

[21]Hollkamp, J. J., and Gordon, R. W., "Modal Testing of a Bladed Disk," *Shock and Vibration Digest*, Vol. 32, No. 1, 2000, p. 56.

[22]Lomenzo, R. A., Barker, A. J., and Wicks, A. L., "Laser Vibrometry System for Rotating Bladed Disks," *Shock and Vibration Digest*, Vol. 32, No. 1, 2000, p. 44.

[23]Fan, Y. C., Ju, M. S., and Tsuei, Y. G., "Experimental Study on Vibration of a Rotating Blade," *Transactions of the ASME*, Vol. 116, No. 3, 1994, pp. 672–677.

[24]Nava, P., Paone, N., Rossi, G. L., and Tomasini, E. P., "Design and Experimental Characterization of a Nonintrusive Measurement System of Rotating Blade Vibration," *Journal of Engineering for Gas Turbines and Power*, Vol. 116, No. 3, 1994, pp. 657–662.

[25]Heath, S., "A Survey of Blade Tip-Timing Measurement Techniques for Turbomachinery Vibration," *Journal of Engineering for Gas Turbines*, Vol. 120, No. 4, 1998, pp. 784–791.

[26]Srinivasan, A. V., Cutts, D. G., and Sridhar, S., "Turbojet Engine Blade Damping," NASA CR 165406, July 1981.

[27]Gordon, R. W., and Hollkamp, J. J., "An Internal Damping Treatment for Gas Turbine Blades," *Proceedings of the 38th AIAA/ASME/ASCE/AHS/ASC Structures, Structural Dynamics, and Materials Conference and Exhibit*, AIAA-Reston, VA, 1997, pp. 442–451.

[28]Gordon, R. W., and Hollkamp, J. J., "An Experimental Investigation of Non-Uniform Damping in Blade-Disk Assemblies," AIAA Paper 98-3747, July 1998.

[29]Oppenheim, A. V., and Schafer, R. W., *Discrete-Time Signal Processing*, Prentice–Hall, Upper Saddle River, NJ, 1989, p. 556.

[30]Coppolino, R. N., "A Simultaneous Frequency Domain Technique for Estimation of Modal Parameters from Measured Data," Aerospace Congress & Exposition, Oct. 1981.

C. Pierre
Associate Editor